Ab Initio Studies on Nanoscale Friction between Fluorinated Diamond Surfaces: Effect of Model Size and Level of Theory

Raisa Neitola and Tapani A. Pakkanen*

Department of Chemistry, University of Joensuu, Post Office Box 111, FI-80101, Joensuu, Finland

Received: May 17, 2006; In Final Form: June 15, 2006

Interactions between two fluorinated diamond surfaces placed in contact with each other were investigated with quantum chemical Hartree−Fock and Møller−Plesset perturbation theory and basis sets def-SV(P), def-TZVP, and 6-31G*. Two models, $C_6H_6F_3-C_{24}H_{24}F_{12}$ and $C_{13}H_{16}F_6-C_{22}H_{24}F_{10}$, were used to examine how model size and level of theory affect the atomic-scale friction, especially the coefficient of friction. Also of interest was a comparison of the interaction energies of the two models with different stacking configurations. The averages of the calculated friction coefficients fell within the range of values 0.28−0.43.

1. Introduction

Development of experimental techniques such as atomic force microscopy, scanning force microscopy, and friction force microscopy along with progress in theoretical methods are offering powerful tools for the study of interacting surfaces and friction processes on atomic scale.[1,2] Present-day nanotechnology requires unique physical and frictional properties of materials that are used in tribological environments, for example, magnetic storage, the aerospace industry, and high-temperature turbine engines. Understanding of the friction between modified surfaces is thus of wide importance. Many groups have focused on thin film lubricants, especially on fluorinated materials, which exhibit extremely low coefficient of friction, low critical surface tension, and high thermal and mechanical stability.[3−10] Teflon is a typical example of a material that, because of its extraordinary frictional properties, has been widely used as an engineering plastic and in highly demanding applications.[11−17] Correspondingly, perfluoropolyether and other perfluorocompounds are of interest for their potential to provide low friction and wear during sliding.[18−22]

Fluorinated diamond and diamond-like carbon (DLC) films are attracting wide attention for their unique combination of extreme hardness, chemical inertness, very low friction, and low wear. Studies by various methods on the effect of fluorination on DLC films[23−25] suggest that fluorination decreases the coefficient of friction by making the films more graphitic. Although there are several studies[26−30] on atomic-scale friction between diamond surfaces, our understanding of the underlying mechanism of nanoscale friction is insufficient for understanding the effects of fluorination on diamond surfaces.

Understanding of nanoscale friction of modified surfaces is of central importance in tribological studies. Accordingly, we carried out ab initio calculations of friction between fluorinated diamond surfaces. Since our earlier investigations[31−33] showed quantum chemical methods to provide an appropriate tool for the examination of atomic-scale friction, we chose the Hartree−Fock (HF) level of theory and the Møller−Plesset (MP) perturbation theory[34] to calculate friction force and the friction coefficient of fluorinated diamond surfaces, as well as to test for adequate model size and level of theory. The specific aim of our study was to explore the nature and consequences of the interactions between fluorine atoms adsorbed on diamond (111) surfaces.

2. Computational Details and Models

2.1. Computational Details. Calculations were carried out with Hartree−Fock (HF) level of theory and Møller−Plesset (MP) perturbation theory. Although Hartree−Fock theory fails to adequately represent electron correlation, it proved in our previous work[31−33] to produce reliable results for friction calculations between two interacting hydrocarbon layers. Second-order Møller−Plesset (MP2) perturbation theory was used to obtain improvement in the description of electron correlation and HF interaction energies. We tested def-SV(P)[35] and def-TZVP[36] basis sets. The differences in interaction energies between def-SVP and def-TZVP basis sets were only a few kilojoules per mole, although the larger basis set (def-TZVP) required at least 3 times more CPU time. Because geometry optimizations with the MP2 method are time-consuming and computationally demanding, all optimizations were performed with basis set def-SV(P), which corresponds to basis set 6-31G* used in our previous studies. Basis set superposition error (BSSE) was taken into account in all calculations and eliminated by counterpoise method.[37,38] The interaction energy, $\Delta E(r)$, of two fluorinated diamond surfaces A and B at distance r was calculated as

$$\Delta E(r) = E^{AB}(r) - E^{A} - E^{B}$$

where the total energy of the double-layer system is $E^{AB}(r)$, and E^{A} and E^{B} are the energies of the separate diamond layers. Geometry optimizations and the energy calculations were performed mainly with the Turbomole 5.8 Program Package[39] by use of the efficient resolution of the identity (RI) technique.[40,41] A few calculations were done with the Gaussian 03 quantum chemistry software.[42]

2.2. Models. Diamond structure is based on tetrahedrally coordinated carbon atoms, which are linked with each other through pure covalent bonding forces. All six-membered carbon rings, analogous to those in cyclohexene in chair conformation, are formed by the overlap of sp^3 hybridization. Figure 1 presents the structure of cubic diamond with staggered layers (ABCA)

10.1021/jp063008p CCC: $33.50
Published on Web 07/27/2006

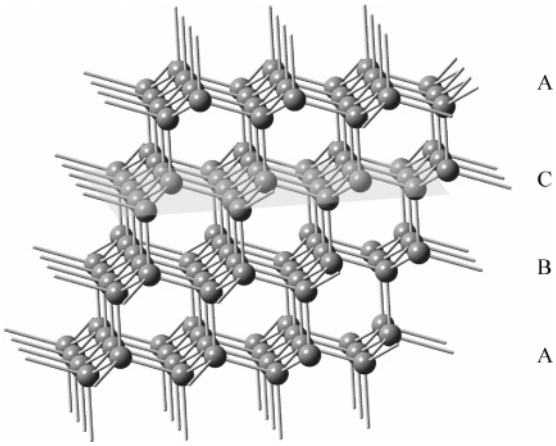

Figure 1. Structure of diamond with the cleavage plane (111).

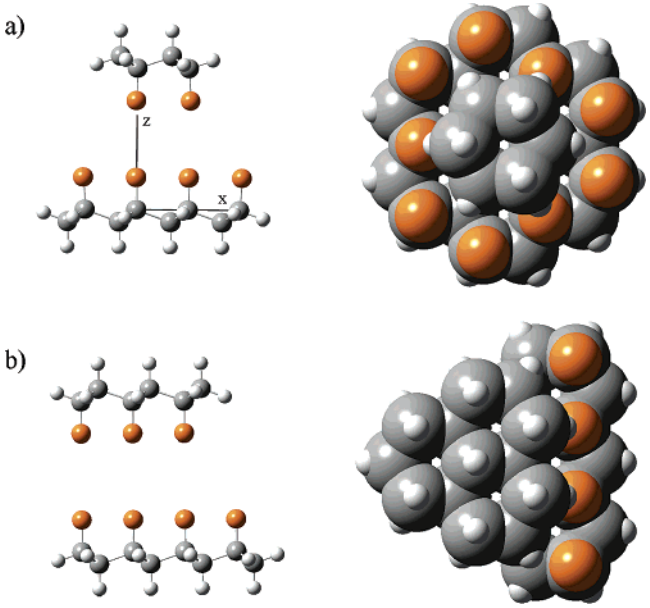

Figure 2. Diamond models, $C_6H_6F_3-C_{24}H_{24}F_{12}$ (a) and $C_{13}H_{16}F_6-C_{22}H_{24}F_{10}$ (b), viewed from the side (ball-and-stick) and the top (space-filling). Dark gray spheres represent carbon atoms; light gray spheres, hydrogen atoms; and orange spheres, fluorine atoms.

and the (111) cleavage plane. Diamond (111) surfaces are a better choice for friction studies than (110) and (100) surfaces because, with fewer bonds needing to be broken, they are more easily cleaved.[43] Furthermore, the diamond (111) surface has a sufficient number of ideal sites for adsorption of fluorine atoms.

Diamond models used in this work were constructed on the basis of information found in the literature:[43−46] the interatomic C−C distances were set at 1.54 Å and bond angles at 109.47° in accordance with the tetrahedrally coordinated structure. Two surface models of different size, $C_6H_6F_3-C_{24}H_{24}F_{12}$ and $C_{13}H_{16}F_6-C_{22}H_{24}F_{10}$, were used to study nanoscale friction between fluorinated diamond surfaces. The models were chosen to maintain the symmetry in sliding. The $C_6H_6F_3-C_{24}H_{24}F_{12}$ model, shown in Figure 2a, was constructed of two fluorinated diamond layers, the upper layer consisting of one six-membered ring and the bottom layer of six six-membered rings. The larger two-layer model, $C_{13}H_{16}F_6-C_{22}H_{24}F_{10}$, is shown in Figure 2b. To eliminate border effects, both models were terminated with hydrogen atoms. The diamond surface models were designed to be symmetrical in all directions as well as to be as large as possible while remaining computationally feasible. In all

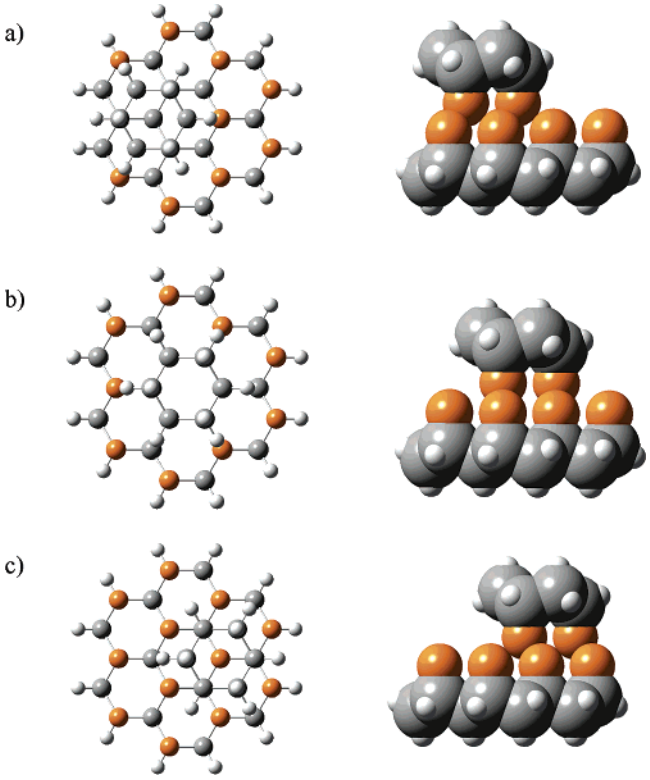

Figure 3. Initial structures of fluorinated diamond surfaces, $C_6H_6F_3-C_{24}H_{24}F_{12}$, in interaction at distance between the layers 4 Å. Dark gray spheres represent carbon atoms; light gray spheres, hydrogen atoms; and orange spheres between the surfaces, fluorine atoms. The upper surface is successively moved to the right: (a) 0 Å (starting point, staggered configuration), (b) 1.46 Å (midpoint, eclipsed configuration), and (c) 2.91 Å (final point, staggered configuration).

calculations the diamond layers were kept frozen, while fluorine atoms between surfaces were optimized.

3. Results and Discussion

3.1. Sliding Contact of Fluorinated Diamond Surfaces. Fluorinated diamond surfaces were placed in sliding contact to obtain insight into interaction and friction between the surfaces. The smaller model ($C_6H_6F_3-C_{24}H_{24}F_{12}$) was used to investigate the sliding process at two distances between diamond surfaces, namely, 4.0 and 5.0 Å. The distance was defined as the distance between nearest carbon layers, and two distances were chosen to describe two types of sliding interaction. At the distance of 4 Å the interactions between fluorine atoms are substantially stronger than those at the distance of 5 Å, since the fluorine atoms brushed heavily against each other. The role of geometry optimization was crucial at the closer distance. The sliding process was modeled by moving the upper surface to the right (along the *x*-axis) in 10 steps of 0.29 Å each, and the geometries of the fluorine atoms were optimized for each step. In the starting configuration, as well as at the final point of sliding, the fluorine atoms of the upper surfaces were situated above the center of the six-membered rings of the underlying surfaces (staggered form). At the halfway point of the sliding process, the fluorine atoms of the different surfaces were face-to-face (eclipsed form). The sliding process is illustrated in Figure 3.

Figure 4 presents the interaction energies between fluorinated diamond surfaces in sliding contact for the $C_6H_6F_3-C_{24}H_{24}F_{12}$ model. For all calculated cases, interaction energies were nearly the same at the starting and final points, where the fluorine atoms were situated top to top. Interaction energy values were highest

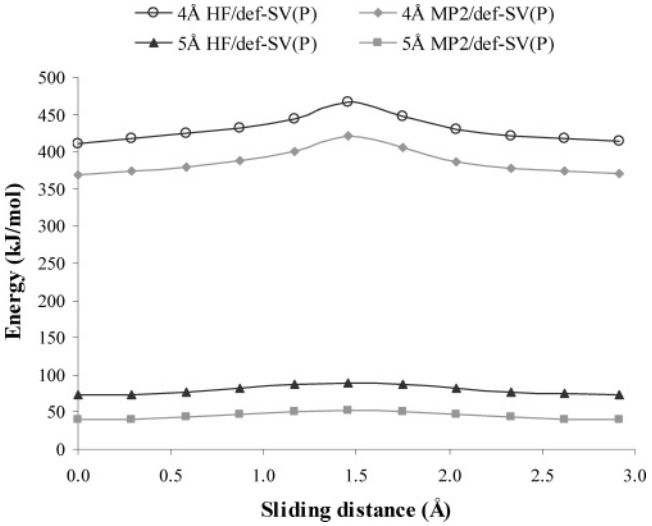

Figure 4. Interaction energy curves in sliding contact for $C_6H_6F_3-C_{24}H_{24}F_{12}$ model calculated with HF/def-SV(P) and MP2/def-SV(P) methods at distances of 4 and 5Å between fluorinated diamond surfaces.

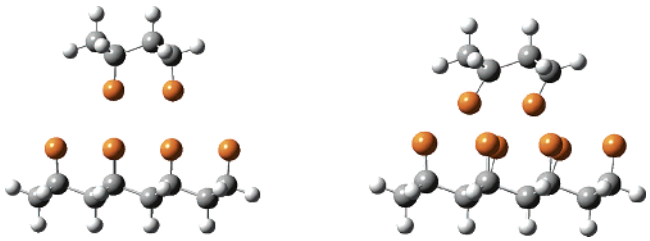

Figure 5. Optimized structures of $C_6H_6F_3-C_{24}H_{24}F_{12}$ model at sliding distance of 1.46 Å. The distances between fluorinated diamond surfaces are 5.0 and 4.0 Å.

at the sliding distance of 1.46 Å, which corresponds to the eclipsed configuration. Comparison of the interaction energies at different levels of theory showed lower interaction energies with the correlated MP2 method than with the HF method, and the magnitude of the difference was nearly the same for the two distances. At the greater distance, where forces were weak, MP2 interaction energies were only half those with HF. As expected, the different type of contact between the fluorine atoms at the two distances caused a notable energy difference (350 ± 30 kJ/mol), at both MP2/def-SV(P) and HF/def-SV(P) levels of theory. Furthermore, the small difference between minimum and maximum (15 kJ/mol) energies at the larger distance (compared with ~50 kJ/mol at the shorter distance) indicated that sliding occurs easily. The repulsion between two diamond surfaces was stronger at a distance of 4 Å because the fluorine atoms rub against each other. The rubbing forced the fluorine atoms to bend as much as 30° from the original tetrahedral orientation, especially at the middle point where the fluorine atoms tried to avoid the top to top situation. Figure 5 presents the optimized structures of fluorinated diamond surfaces at distances 5 and 4 Å.

3.2. Fluorinated Diamond Surfaces Pressed to Close Contact. In addition to the interaction energies for sliding contact, interaction energies for the case in which the surfaces are pressed to close contact are needed for calculation of the friction force and coefficient of friction between two interacting surfaces. In the next set of calculations, carried out with both $C_6H_6F_3-C_{24}H_{24}F_{12}$ and $C_{13}H_{16}F_6-C_{22}H_{24}F_{10}$ models, fluorinated diamond surfaces were pressed closer against each other in small (0.25 Å) steps so that the distance between the surfaces decreased from 6 to 3.5 Å. Both staggered and eclipsed configurations were studied, since the investigation of the sliding

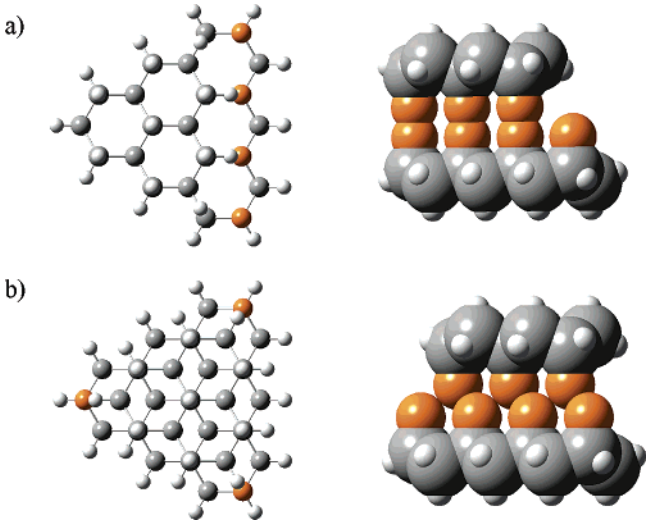

Figure 6. Initial structures of fluorinated diamond surfaces, $C_{13}H_{16}F_6-C_{22}H_{24}F_{10}$, in interaction at distance between the layers 4 Å. Dark gray spheres represent carbon atoms; light gray spheres, hydrogen atoms; and orange spheres between the surfaces, fluorine atoms. The upper surface is successively moved to the right: (a) 0 Å (eclipsed configuration) and (b) 2.91 Å (staggered configuration).

process showed these two stacking configurations to correspond to the minimum and the maximum interaction energies in sliding contact. Figure 3 panels a and b show the orientations of pressing for the smaller model, and Figure 6 panels a and b show those for the larger model. Interaction energies and geometry optimization were calculated at both HF/def-SV(P) and MP2/def-SV(P) levels of theory. Additionally, for the staggered orientation we tested basis sets def-TZVP and 6-31G* at a few optimization points to obtain more exact information about the reliability of the different basis sets.

The interaction energy curves for the staggered and eclipsed configurations are presented in Figures 7 and 8. Three clear trends can be seen in the figures. First, the interaction energies for the $C_{13}H_{16}F_6-C_{22}H_{24}F_{10}$ model are higher than those for the smaller model, $C_6H_6F_3-C_{24}H_{24}F_{12}$. Second, as we found in the sliding case, the interaction energies for the eclipsed configurations are higher than those for the staggered configuration except for short distances between layers. Both these trends are a consequence of the greater repulsive interaction between the surfaces. Third, because of the greater repulsive interaction, the interaction energies mostly increased when the surfaces were pressed closer against each other. At short distances between fluorinated diamond surfaces, from 3.5 to 4.0 Å, optimization of the fluorine atoms played a crucial role because the surfaces became "flattened" against each other, particularly in the eclipsed configuration. When the fluorine atoms were pressed in close proximity to each other, they bent to avoid face-to-face contact, with the result that the interaction energies stabilized or even decreased. More precisely, the deflection of the curves was not simultaneous and it was more pronounced for the larger model. Visualization of the geometries of the fluorine atoms at the deflection points shows the reason for the differences in the energy curves (Figures 5 and 9). Optimization of the $C_{13}H_{16}F_6-C_{22}H_{24}F_{10}$ model at the distance of 3.75 Å allowed some of the fluorine atoms to distort so that they slipped away from the bottom surface and caused a decrease in the energy. This kind of distortion was not possible for the $C_6H_6F_3-C_{24}H_{24}F_{12}$ model since, although the fluorine atoms of the upper surface bent, they remained over the top of the bottom layer. In the case of the $C_{13}H_{16}F_6-C_{22}H_{24}F_{10}$ model,

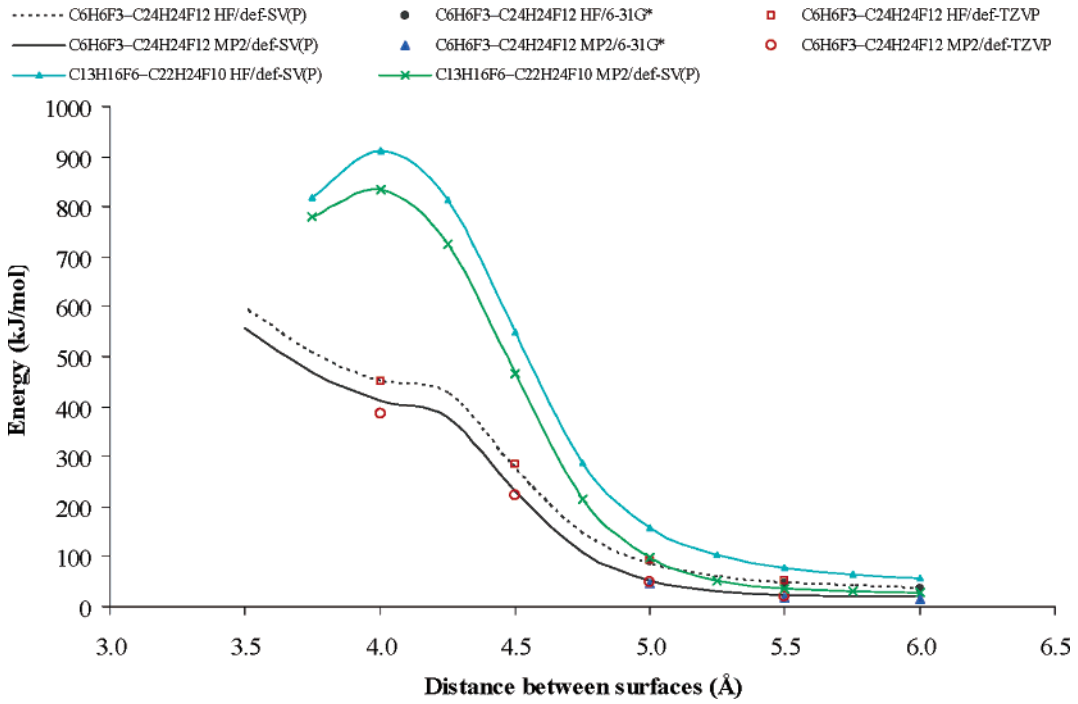

Figure 7. Comparison of interaction energies *E* (kilojoules/mole) for eclipsed $C_6H_6F_3-C_{24}H_{24}F_{12}$ and $C_{13}H_{16}F_6-C_{22}H_{24}F_{10}$ models calculated at HF/def-SV(P), HF/6-31G*, HF/def-TZVP, MP2/def-SV(P), MP2/6-31G*, and MP2/def-TZVP levels of theory.

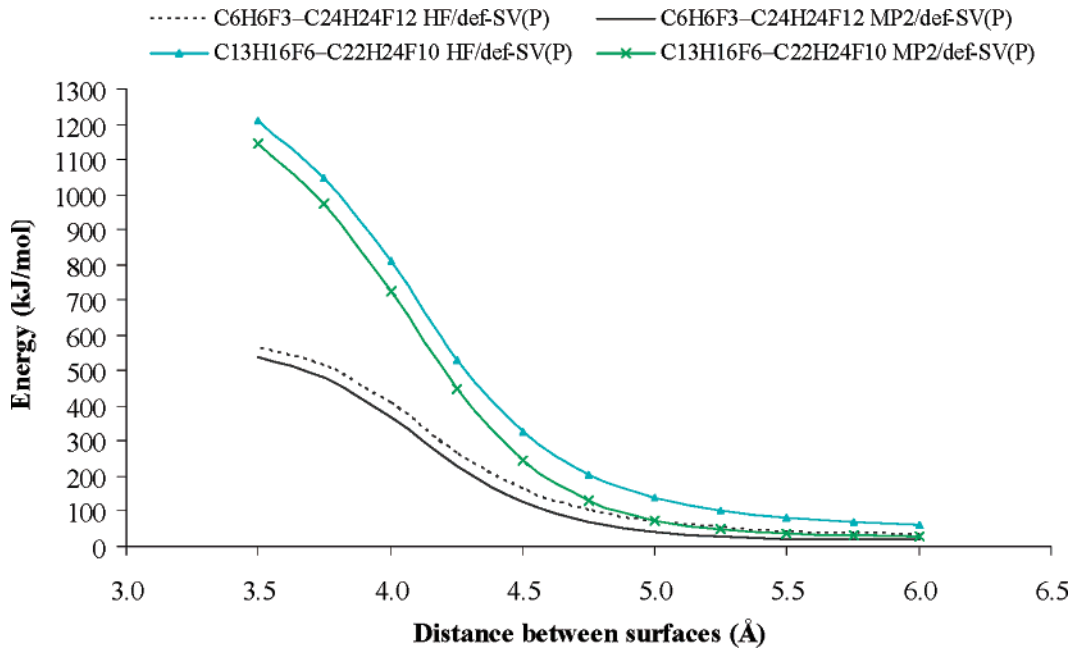

Figure 8. Comparison of interaction energies *E* (kilojoules/mole) for staggered $C_6H_6F_3-C_{24}H_{24}F_{12}$ and $C_{13}H_{16}F_6-C_{22}H_{24}F_{10}$ models calculated at HF/def-SV(P) and MP2/def-SV(P) levels of theory.

the "overhanging" at short distances between the surfaces could be eliminated with a larger bottom layer.

Besides studying the influence of the model size and the surface configuration, we investigated how different levels of theory affect the interaction between two fluorinated diamond surfaces. We calculated interaction energies for both models with HF/def-SV(P) and MP2/def-SV(P) and eclipsed and staggered configurations. Furthermore, a closer study was made of the eclipsed configuration by calculating the interaction energies using both Gaussian 03 with HF/6-31G* and MP2/6-31G* and Turbomole 5.8 with HF/def-TZVP and MP2/def-TZVP. Because the ab initio calculations are very time-consuming, especially with the traditional MP2 method and def-TZVP basis set, we calculated only a few points at different distances between surfaces. As before, the interaction energies calculated with the MP2 level of theory were lower than those calculated with the HF method. The relative difference in energy ranged from 20 to 80 kJ/mol depending on the model size and the distance between the diamond surfaces. In contrast, energies obtained with the 6-31G* and def-TZVP basis sets deviated only a few kilojoules per mole from those calculated with def-SV(P). The benefit of a larger basis set seemed to be inconsequential. In other words, the smaller def-SV(P) basis set appeared to be capable of modeling atomic-scale friction between two interacting surfaces. The BSSE corrections also seemed to be only slightly higher with the smaller basis set:

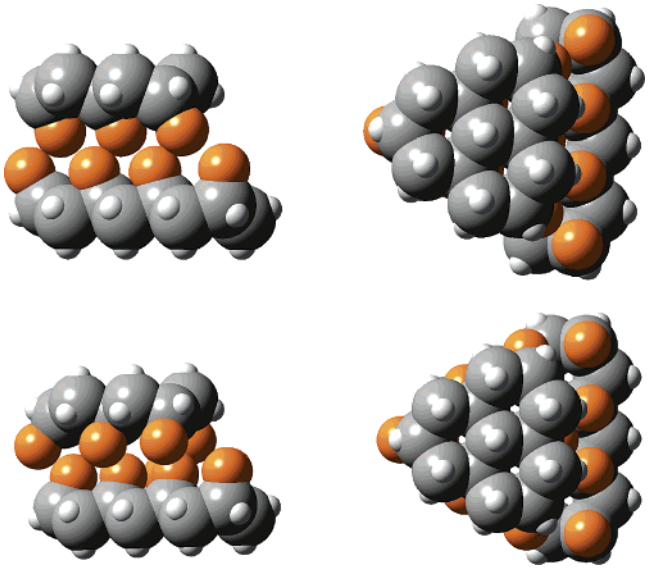

Figure 9. Optimized structures of fluorinated diamond $C_{13}H_{16}F_6-C_{22}H_{24}F_{10}$ model under pressing. Distance between layers: (top) 3.75 Å; (bottom) 4.0 Å.

BSSE correction for the $C_6H_6F_3-C_{24}H_{24}F_{12}$ model was about 10% with HF/def-SV(P) and about 5% with HF/def -TZVP. However, the influence of the BSSE correction on the interaction energies at MP2 level of theory was notable; the proportion varied from 20% to 40%.

3.3. Coefficient of Friction. The final objective of our nanoscale friction studies was to calculate the friction force and the coefficient of friction. The coefficient of friction is the friction force divided by the normal load. In the following, we present the coefficient of friction calculated by the procedure of Zhong and co-workers.[47−50] First, a polynomial function was fitted to the curve of interaction energy (Figures 7 and 8) and the function was differentiated to obtain the normal load, F_N. Only the interaction energies when the fluorinated diamond surfaces were between 6.0 and 4.25 Å apart were considered. The friction force in atomic scale under normal load was then obtained by calculating the energy difference between the eclipsed and staggered configurations (minimum and maximum) and dividing this by the difference in distance between the minimum and maximum values.

For both models, the friction force increased almost linearly with the increase of the normal load, which is in agreement with Amontons' law[1] of friction. Figure 10 presents a comparison of the friction force for the fluorinated diamond models with the friction force for diamond surfaces calculated in our earlier investigation.[31] Friction force was higher for the $C_{13}H_{16}F_6-C_{22}H_{24}F_{10}$ model because there were more F−F interactions between the surfaces and the repulsion between the diamond surfaces was thus larger. Similarly, we can conclude that the steric interactions between fluorinated diamond surfaces increased the friction force over that of hydrogenated diamond surfaces. These observations are in agreement with the results of investigations of fluorinated self-assembled monolayers.[3,6,8,9] For example, Kim et al.[6] studied steric interactions, changes in film order, and molecular motion and observed greater friction for CF_3-terminated alkyl chains than the fully hydrogenated analogue. In contrast to this, the results of Yamada[19] indicated that surface configurations of fluorinated ether films flatten slightly in sliding interactions at high pressure, lowering the friction coefficient. Similarly, studies of fluorinated diamond films[23,24,26] suggested that fluorine improves the friction properties since it decreases the surface energy as the films become more graphitized. In this work, modification of the surface structure did not substantially affect the friction because only the movement of fluorine atoms was permitted and the surface became flattened only at close distances between the diamond surfaces (<4 Å).

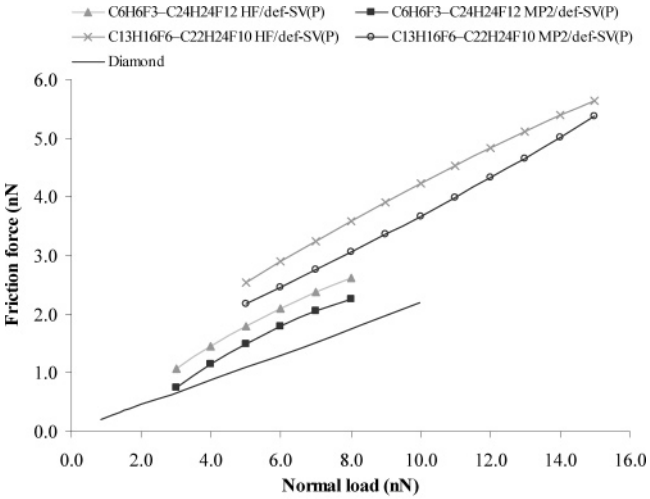

Figure 10. Friction force as a function of normal load for $C_6H_6F_3-C_{24}H_{24}F_{12}$ and $C_{13}H_{16}F_6-C_{22}H_{24}F_{10}$ models calculated with HF/def-SV(P) and MP2/def-SV(P) levels of theory. The friction force for diamond surface[31] is included for comparison.

TABLE 1: Calculated Coefficients of Friction for Fluorinated Diamond Models and Average Values for the Different Models and Levels of Theory

	$C_6H_6F_3-C_{24}H_{24}F_{12}$		$C_{13}H_{16}F_6-C_{22}H_{24}F_{10}$	
normal load (nN)	HF/def-SV(P)	MP2/def-SV(P)	HF/def-SV(P)	MP2/def-SV(P)
3.00	0.36	0.25		
4.00	0.36	0.29		
5.00	0.36	0.30	0.51	0.43
6.00	0.35	0.30	0.48	0.41
7.00	0.34	0.29	0.46	0.39
8.00	0.33	0.28	0.45	0.38
9.00			0.43	0.37
10.00			0.42	0.37
11.00			0.41	0.36
12.00			0.40	0.36
13.00			0.39	0.36
14.00			0.38	0.36
15.00			0.38	0.36
avg	0.35	0.28	0.43	0.38

The calculated coefficients of friction are summarized in Table 1. The coefficients of friction were lower with MP2/def-SV(P) than HF/def-SV(P) and lower for the $C_6H_6F_3-C_{24}H_{24}F_{12}$ model than for the $C_{13}H_{16}F_6-C_{22}H_{24}F_{10}$ model. The difference between the models is probably the result of the different surface packing and number of interacting fluorine atoms. Thus, there are six direct face-to-face contacts between fluorine atoms in the $C_{13}H_{16}F_6-C_{22}H_{24}F_{10}$ model and only three in the $C_6H_6F_3-C_{24}H_{24}F_{12}$ model. The average values of the coefficients of friction at normal load 3−15 nN varied from 0.28 to 0.43.

4. Conclusions

Our investigation of atomic-scale friction between two fluorinated diamond surfaces comprised calculation of friction forces and coefficients of friction as well as examination of the effects of model size and level of theory on friction. Interaction energies between two fluorinated diamond surfaces for $C_6H_6F_3-C_{24}H_{24}F_{12}$ and $C_{13}H_{16}F_6-C_{22}H_{24}F_{10}$ models were calculated at

HF and MP2 levels of theory by use of basis sets def-SV(P), 6-31G*, and def-TZVP.

Interaction energies increased as the repulsive interactions between fluorine atoms became stronger, that is, when the surfaces were pressed into closer proximity and when the number of fluorine atoms (size of the model) increased. As expected, the interaction energies obtained with the MP2/def-SV(P) method were lower than those obtained with HF/def-SV(P). The differences in the results with the def-SV(P), 6-31G*, and def-TZVP basis sets were almost negligible.

For all calculated cases, friction force increased almost linearly with increase of the normal load, which suggests that Amontons' law is also obeyed on the atomic scale. The calculated average values of the friction coefficient varied from 0.28 to 0.43 depending on model size and level of theory. In many investigations, including this work, bulkier fluorine atoms have been found to cause more steric interaction between two surfaces than do hydrogen atoms and thus to increase the friction force and the coefficient of friction between two diamond surfaces.

References and Notes

(1) Bhushan, B. *Introduction to Tribology*; John Wiley & Sons: New York, 2002.

(2) Bhushan, B. *Modern Tribology Handbook I−II*; CRC Press: Boca Raton, FL, 2001.

(3) Li, S.; Cao, P.; Colorado, R.; Yan, X.; Wenzl, I.; Shmakova, O. E.; Graupe, M.; Lee, R.; Perry, S. S. *Langmuir* **2005**, *21*, 933.

(4) Yamada, S.; Israelachvili, J. *J. Phys. Chem. B* **1998**, *102*, 234.

(5) Lorenz, C. D.; Webb, E. B.; Stevens, M. J.; Chandross, M.; Grest, G. S. *Tribol. Lett.* **2005**, *19*, 93.

(6) Kim, H. I.; Koini, T.; Lee, T. R.; Perry, S. S. *Tribol. Lett.* **1998**, *4*, 137.

(7) DePalma, V.; Tillman, N. *Langmuir* **1989**, *5*, 868.

(8) Overney, R. M.; Meyer, E.; Frommer, J.; Güntherodt, H.-J. *Langmuir* **1994**, *10*, 1281.

(9) Chaudhury, M. K.; Owen, M. *Langmuir* **1993**, *9*, 29.

(10) Fan, F.; Li, X.-D.; Miyashita, T. *Thin Solid Films* **1999**, *348*, 238.

(11) Breiby, D. W.; Sølling, T. I.; Bunk, O.; Nyberg, R. B.; Norrman, K.; Nielsen, M. M. *Macromolecules* **2005**, *38*, 2383.

(12) Sui, H.; Pohl, H.; Schomburg, U.; Upper, G.; Heine, S. *Wear* **1999**, *224*, 175.

(13) Chen, W. X.; Li, F.; Han, G.; Xia, J. B.; Wang, L. Y.; Tu, J. P.; Xu, Z. D. *Tribol. Lett.* **2003**, *15*, 275.

(14) Marx, S.; Junghans, R. *Wear* **1996**, *193*, 253.

(15) Schönherr, H.; Vancso, J. *Polymer* **1998**, *39*, 5705.

(16) Briscoe, B. J.; Yao, L. H.; Stolarski, T. A. *Wear* **1986**, *108*, 357.

(17) Holmberg, K.; Wickström, G. *Wear* **1987**, *115*, 95.

(18) Choi, J.; Kawaguchi, M.; Kato, T. *IEEE Trans. Magn.* **2003**, *39*, 2492.

(19) Yamada, S. *Langmuir* **2005**, *21*, 8724.

(20) Tsuboi, H.; Kishii, N.; Kamei, T.; Kurihara, K.; Kobayashi, K.; Iwamoto, Y. *Tribol. Int.* **2003**, *36*, 417.

(21) Laschitsch, A.; Bailey, L. E.; Tyndall, G. W.; Frank, C. W.; Johannsmann, D. *Appl. Phys. Lett.* **2001**, *78*, 2601.

(22) Cheong, C. U.; Stair, P. C. *Tribol. Lett.* **2001**, *10*, 117.

(23) Miyake, S. *Appl. Phys. Lett.* **1994**, *9*, 1109.

(24) Yu, G. Q.; Tay, B. K.; Sun, Z.; Pan, L. K. *Appl. Surf. Sci.* **2003**, *219*, 228.

(25) Tambe, N.; Bhushan, B. *Scr. Mater.* **2005**, *52*, 751.

(26) Nakamura, T.; Suzuki, M.; Ishihara, M.; Ohana, T.; Tanaka, A.; Koga, Y. *Langmuir* **2004**, *20*, 5846.

(27) Tanaka, A.; Umeda, K.; Takatsu, S. *Wear* **2004**, *257*, 1096.

(28) Bhushan, B.; Liu, H.; Hsu, S. M. *J. Tribol.* **2004**, *126*, 583.

(29) Prioli, R.; Jacobsohn, L. G.; Maia da Costa, M. E. H.; Freire, F. L. *Tribol. Lett.* **2003**, *15*, 177.

(30) Harrison, J. A.; Perry, S. S. *MRS Bull.* **1998**, *23*, 27 and references therein.

(31) Neitola, R.; Pakkanen, T. A. *J. Phys. Chem. B* **2001**, *105*, 1338.

(32) Neitola, R.; Pakkanen, T. A. *Chem. Phys.* **2004**, *299*, 47.

(33) Neitola, R.; Pakkanen, T. A. *J. Phys. Chem. B* **2005**, *109*, 10348.

(34) Szabo, A.; Ostlund, N. S. *Modern Quantum Chemistry: Introduction to Advanced Electronic Structure Theory*, Macmillan Publishing Co., Inc.: New York, 1982.

(35) Schäfer, A.; Horn, H.; Ahlrichs, R. *J. Chem. Phys.* **1992**, *97*, 2571.

(36) Schäfer, A.; Huber, C.; Ahlrichs, R. *J. Chem. Phys.* **1994**, *100*, 5829.

(37) Scheiner, S. *Molecular Interactions*; John Wiley & Sons: New York, 1997.

(38) Kestner, N.; Combariza, J. In *Reviews in Computational Chemistry*; Lipkowitz, K. B., Boyd, D. B., Eds.; John Wiley & Sons: New York, 1999.

(39) Ahlrichs, R.; Bär, M.; Häser, M.; Horn, H.; Kölmel, C. *Chem. Phys. Lett.* **1989**, *162*, 165.

(40) Weigend, F.; Häser, M. *Theor. Chem. Acc.* **1997**, *97*, 331.

(41) Weigend, F.; Häser, M.; Petzelt, H.; Ahlrichs, R. *Chem. Phys. Lett.* **1998**, *294*, 143.

(42) Frisch, M. J.; Trucks, G. W.; Schlegel, H. B.; Scuseria, G. E.; Robb, M. A.; Cheeseman, J. R.; Montgomery, J. A., Jr.; Vreven, T.; Kudin, K. N.; Burant, J. C.; Millam, J. M.; Iyengar, S. S.; Tomasi, J.; Barone, V.; Mennucci, B.; Cossi, M.; Scalmani, G.; Rega, N.; Petersson, G. A.; Nakatsuji, H.; Hada, M.; Ehara, M.; Toyota, K.; Fukuda, R.; Hasegawa, J.; Ishida, M.; Nakajima, T.; Honda, Y.; Kitao, O.; Nakai, H.; Klene, M.; Li, X.; Knox, J. E.; Hratchian, H. P.; Cross, J. B.; Adamo, C.; Jaramillo, J.; Gomperts, R.; Stratmann, R. E.; Yazyev, O.; Austin, A. J.; Cammi, R.; Pomelli, C.; Ochterski, J. W.; Ayala, P. Y.; Morokuma, K.; Voth, G. A.; Salvador, P.; Dannenberg, J. J.; Zakrzewski, V. G.; Dapprich, S.; Daniels, A. D.; Strain, M. C.; Farkas, O.; Malick, D. K.; Rabuck, A. D.; Raghavachari, K.; Foresman, J. B.; Ortiz, J. V.; Cui, Q.; Baboul, A. G.; Clifford, S.; Cioslowski, J.; Stefanov, B. B.; Liu, G.; Liashenko, A.; Piskorz, P.; Komaromi, I.; Martin, R. L.; Fox, D. J.; Keith, T.; Al-Laham, M. A.; Peng, C. Y.; Nanayakkara, A.; Challacombe, M.; Gill, P. M. W.; Johnson, B.; Chen, W.; Wong, M. W.; Gonzalez, C.; Pople, J. A. *Gaussian 03*, Revision C.02; Gaussian, Inc.: Wallingford, CT, 2004.

(43) Jakubke, H.-D.; Jeschkeit, H. *Concise Encyclopedia Chemistry*; Walter de Gruyter & Co.: Berlin, 1993.

(44) Lee, J. D. *Concise Inorganic Chemistry*, 5th ed.; Blackwell Science Ltd.: Oxford, U.K., 1996.

(45) Borg, R. J.; Dienes, G. J. *The Physical Chemistry of Solids*; Academic Press: San Diego, CA, 1992.

(46) Parrish, W. *Acta Crystallogr.* **1960**, *13*, 838.

(47) Zhong, W.; Tománek, D. *Phys. Rev. Lett.* **1990**, *64*, 3054.

(48) Tománek, D.; Zhong, W.; Thomas, H. *Europhys. Lett.* **1991**, *8*, 887.

(49) Overney, G.; Zhong, W.; Tománek, D. *J. Vac. Sci. Technol. B* **1991**, *9*, 479.

(50) Matsuzawa, N. N.; Kishii, N. *J. Phys. Chem. A* **1997**, *101*, 10045.